High Temperature Characterization of Ceramic Pressue Sensors

Michael A. Fonseca, Jennifer M. English, Martin von Arx and Mark G. Allen
Georgia Institute of Technology, School of Electrical and Computer Engineering
Atlanta, GA 30332-0250, USA, gt8456b@prism.gatech.edu

SUMMARY

This work reports functional wireless ceramic micromachined pressure sensors operating at 450 °C, with demonstrated materials and readout capability indicating potential extension to temperatures in excess of 600 °C. These devices are self-packaged and are operating in actual high-temperature environments, not in simulated hot-plate testbeds. A resonant readout technique is employed, in which a planar spiral inductor and a pressure-sensitive capacitor form a passive LC circuit, the resonance frequency of which is sensitive to the external applied pressure, and which can be read out using a simple external loop antenna.

Keywords: Pressure sensor, LTCC, high temperature, ceramic, screen printed, capacitive sensor.

INTRODUCTION

There are many applications, such as in turbine and internal combustion engines, in which the sensing of pressure at high temperatures is required. Several approaches to high temperature pressure sensing, such as approaches based on silicon carbide and optical sensors, have been discussed [1]. An alternative approach is based on movable diaphragm ceramic pressure sensors which are read out using passive wireless approaches. Previous work based on this approach demonstrated sensors operating in temperature ranges from 0-200 °C and pressures of 0-100 bar [2]. These were fabricated using low temperature co-fireable ceramics (LTCC) and electroplated Cu. The measured sensitivity expressed in frequency-shift per pressure difference, was -2.6 MHz bar $^{-1}$. However, the electroplated copper limited the maximum temperature to which the sensor could be exposed. In addition, since the copper was formed on the external surfaces of the ceramic sensor, the metallization was sensitive to oxidation. In this work, we report functional wireless ceramic micromachined pressure sensors, operating at 450 °C, with demonstrated materials and readout capability indicating potential extension to temperatures in excess of 600 °C. These devices are self-packaged and are operating in actual high-temperature environments, not in simulated hot-plate testbeds. Standard ceramic electronic packaging techniques are used to fabricate the sensors. Current sensors are fabricated with LTCC and *embedded* screen-printed high-temperature silver, thereby forming *self-packaged* structures in which only ceramic is exposed to the environment, as illustrated in Fig 1a.

The LTCC sensors are fabricated using multiple sheets of Dupont 951AT ceramic tape [3]. The sensors consist of two diaphragms, separated by a vacuum-sealed cavity of gap size t_g (Fig 1a). If a pressure P is applied, the gap size of the cavity between the two membranes is reduced and the capacitor value increases. The capacitor is electrically connected to a planar spiral inductor coil. These components form a passive LC resonator with resonant frequency f_o, which is pressure dependent. To achieve passive wireless telemetry, the sensor is placed inside an external loop antenna coil and the impedance and phase response of the antenna coil are measured as a function of frequency.

DESIGN AND FABRICATION

The LTCC tape consists of alumina and glass particles suspended in an organic binder. The ceramic tape layers are cut to a size of 40 cm^2 using an IR laser (rated for 10 Watts at 1 kHz). The sensor is comprised of three sections. A circle and/or channel is cut out from the center sections to form the cavity and evacuation channel. For the top and bottom sections, metal conducting ink (silver) is screen printed on the inside of the two outer sheets, which form the pressure sensitive diaphragms. A metal-filled via connection is made between the two coils and the tape is then laminated in a hot press. The sample is then fired at 850 °C to form the final ceramic structure [3]. After firing, glass frit is used to cover the evacuation channel and heated to 790 °C in ambient vacuum, causing the frit to melt and seal the cavity under vacuum. Fig 1b shows a top view of a fabricated sensor. The sensor is backlit allowing the visualization of the embedded conductor lines. Fig 1c is an SEM photomicrograph of a fabricated sensor that has been diced to show the sensor cavity.

MODELING

The electromechanical model of the ceramic pressure sensor is derived as follows. First, the load-deflection relation between the center deflection d_o of the membranes as a function of applied pressure P is determined. Next, the pressure dependent capacitor $C_s(P)$ is calculated as a function of d_o. This capacitance determines the resonant frequency of the sensor. Finally, the coupled electrical system of antenna and sensor is analyzed. The sensor model is illustrated in Fig 2.

The deflection of the diaphragms is calculated using thin plate theory, in which the effects of both bending and stretching of the diaphragm are considered. Several assumptions are made. (*i*) The edges of the diaphragm are clamped and can be modeled by built-in boundary conditions; (*ii*) No residual stress is present in the diaphragms since the diaphragms as well as the rest of the sensor are fabricated from the same material; and (*iii*) The diaphragms are subject to a uniform load P. Using these assumptions and large deflection theory for circular plates the center deflection of the diaphragm is given by:

$$\frac{d_o}{t_m} + 0.488\left(\frac{d_o}{t_m}\right)^3 = \frac{3P(1-\nu^2)}{16E}\left(\frac{a}{t_m}\right)^4, \qquad (1)$$

where a is the plate radius, E is Young's Modulus and ν is Poisson's ratio of the plate [4]. The capacitor C_s for the pressure sensor consists of the top and bottom metal electrodes separated by the cavity and part of the top diaphragm, as shown in Fig 1a. The capacitance at zero pressure is given by

$$C_o = \frac{\varepsilon_o \pi a^2}{t_g + 0.5t_{m1}\varepsilon_r^{-1}} + \frac{\varepsilon_o \varepsilon_r \pi (a_e^2 - a_c^2)}{t_g + 0.5t_{m1}}, \qquad (2)$$

where a_e and a_c are the electrode and cavity radius, respectively, t_{m1} and ε_r are the top diaphragm thickness and relative dielectric constant of the ceramic, respectively .

A pressure dependent capacitor model, for the case when the deflections are small compared with the gap height, is given by:

$$C_s(P) = C_o \sum_{i=0}^{\infty} \frac{1}{2i+1}\left(\frac{d_{o1} + d_{o2} + d_{i1} + d_{i2}}{t_g + 0.5t_{m1}\varepsilon_r^{-1}}\right)^i, \qquad (3)$$

where d_{i1} and d_{i2} are the initial deflections of the plates.

To relate this pressure-dependent capacitance to a frequency shift, the sensor resonance and its coupling to the antenna is modeled as a two-port network using transformer theory, as shown in Fig 2b [5].

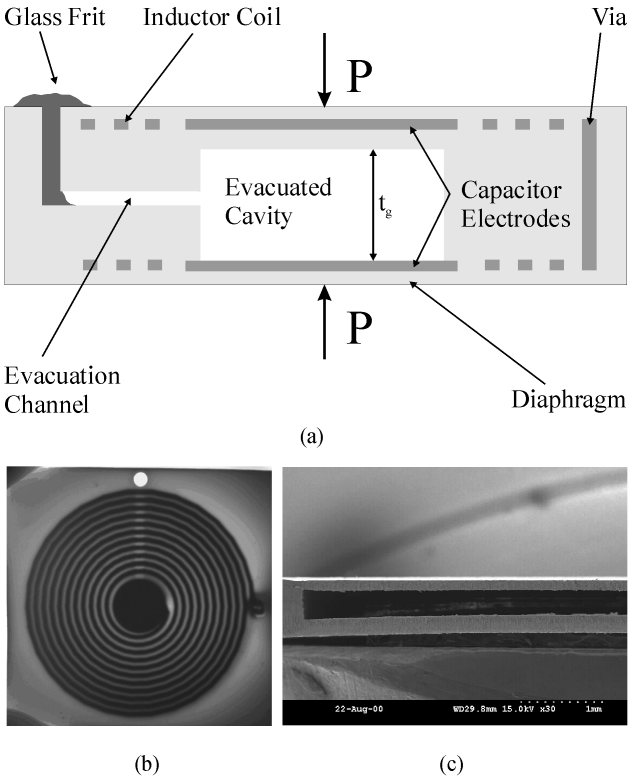

Fig.1: *(a) Ceramic pressure sensor cross sectional view; (b) top view of fabricated device in transmission showing embedded coils; (c) SEM photomicrograph of cavity.*

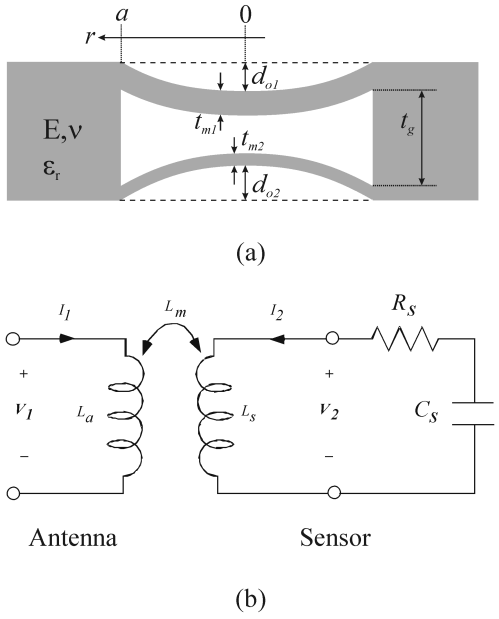

Fig.2: *(a) Schematic cross-section of sealed cavity structure for mechanical modeling; (b) equivalent circuit of electrical model for a sensor coupled with an antenna.*

The input impedance of the antenna is expressed in terms of the parameters of the sensor it encloses:

$$Z_1 = \frac{V_1}{I_1} = j2\pi f L_a \left[1 + k^2 \frac{\left(\frac{f}{f_o}\right)^2}{1 - \left(\frac{f}{f_o}\right)^2 + \frac{1}{Q} j \frac{f}{f_o}} \right]. \qquad (4)$$

This result relates the resonance frequency $f_o = 0.5\pi (LC)^{-.5}$ and $Q = 2\pi f_o L_s/R_s$ of the sensor to the measurable quantity Z_1 and the coupling coefficient $k = L_m(L_a L_s)^{-1/2}$. By measuring Z_1 as a function of f, f_o can be extracted.

RESULTS

Measurements for the pressure sensors were taken using a pressure/temperature vessel. The pressure can be controlled from atmospheric pressure up to 194 bar using a nitrogen gas tank, and the temperature can be controlled from room temperature up to 600 °C. The loop antenna is placed inside the vessel and has an inductance of roughly 670 nH. The frequency dependent antenna impedance is measured using an HP9141A impedance analyzer. Feed-throughs in the vessel shell provide the connections between antenna and impedance analyzer. They have a parasitic cross-coupling capacitance of 0.202 pF. The self-resonance frequency of this system is 43 MHz, which is high enough for our purposes to avoid interaction with the sensor resonance.

The sensors are placed in the plane of the antenna loop and the impedance Z of the antenna is measured as a function of frequency. Fig 3 shows the measured phase and magnitude of Z_1 for sensor at atmospheric pressure. Below and above resonance the phase is close to the ideal value of 90° for an inductor and the magnitude depends linearly on the frequency.

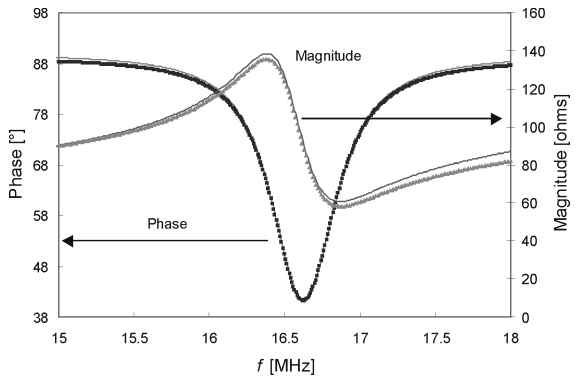

Fig.3: *Phase Φ_1 and magnitude of impedance Z_1 vs. Frequency at 25 °C. The measured data are shown as points while the optimum fit using equation (4) is shown as solid line.*

At resonance, the sensor induces a change in the phase and magnitude of the antenna impedance. The phase data was fit with (4), using Mathematica 4.0. The fit is shown as a solid line in Fig 3. The resonance frequency f_o, the coupling coefficient k, and the quality factor Q obtained from the fit are 16.52 MHz, 0.157, and 36, respectively. Note that the phase minimum f_{min} is 0.6 % higher than f_o. The difference is explained by calculating the frequency at which the phase minimum of Z_1 occurs from (4). The Taylor expansion of f_{min} in k and Q^{-1} is:

$$f_{min} = f_o \left(1 + \frac{k^2}{4} + \frac{1}{8Q^2} \right). \qquad (5)$$

The difference between f_{min} and f_o can therefore be explained as an effect of the coupling factor k in this measurement.

The device was operated up to 450 °C in a pressure range of 1-5 bar. The sensitivity of the sensor ranges between –70 to –245 kHz bar^{-1}. Since no sensor data were taken at ambient vacuum (i.e., ambient pressure of zero bar), the first data points are at 1 bar (Fig 4). In order to compare with the theoretical development,

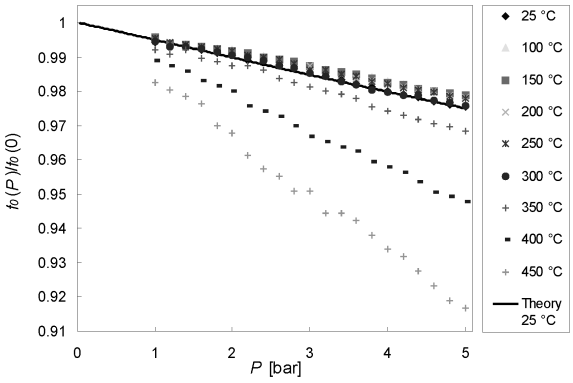

Fig.4: *Normalized resonance frequency fo vs. pressure P. The solid line denotes the theoretical pressure dependence according to model eq. (8).*

which assumes a zero minimum differential pressure (as well as absolute pressure, since the reference pressure sealed in the cavity is ideally zero bar), the experimental data were extrapolated to a pressure of zero bar (yielding a zero pressure resonance frequency $f_o(0)$), and this extrapolated frequency was used to normalize the data points in accordance with the theory. At low pressures, f_o depends approximately linearly on P. The pressure sensitivities of the sensor between 1 and 5 bar range from –70 kHz bar^{-1} (room temperature to 300 °C) to –245 kHz bar^{-1} (450 °C). The theoretical pressure

dependence for f_o was calculated from the model above, yielding:

$$f_o(P) = f_o(P=0)\left(\sum_{i=0}^{\infty}\frac{1}{2i+1}\left(\frac{d_{o1}+d_{o2}+d_{i1}+d_{i2}}{t_g+0.5t_{m1}\varepsilon_r^{-1}}\right)^i\right)^{-\frac{1}{2}} \quad (6)$$

The pressure dependence predicted by theory is shown as a solid line in Fig 4. A linearized sensitivity of –83 kHz/bar over the range 0-5 bar is obtained, in reasonable agreement with the measured data at temperatures below 350 °C.

To determine the parasitic temperature sensitivity, the resonance frequency was measured as a function of temperature. Fig 5 shows normalized resonance frequencies f_o between 25 ºC and 450 ºC. The average slope is –4.6 kHz ºC^{-1} between 25 ºC and 450 ºC. A possible compensation scheme utilizes integration of a second sensor with no pressure dependence on the same substrate, i.e., a sensor without cavity.

Fig 5 also shows the quality factor Q as a function of temperature. Q is reduced from 36 at 25 ºC to 6.5 at 450 ºC, which limits the range of operation of sensors fabricated from these materials.

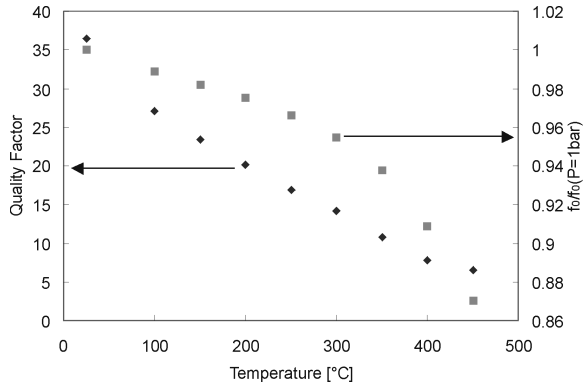

Fig.5: *Normalized quality factor Q and resonant frequency fo versus temperature*

CONCLUSION AND OUTLOOK

Looking toward higher operating temperatures, alternate ceramic materials and metallizations for operation at high temperature have been characterized. The high temperature ceramic (alumina tape) consists solely of alumina particles and organic binder (i.e., no glass filler), and is typically fired at temperatures in excess of 1400 °C. Structures have been fabricated from this material with embedded screen-printed Pt metallization as described above (Fig 1). Successful detection of

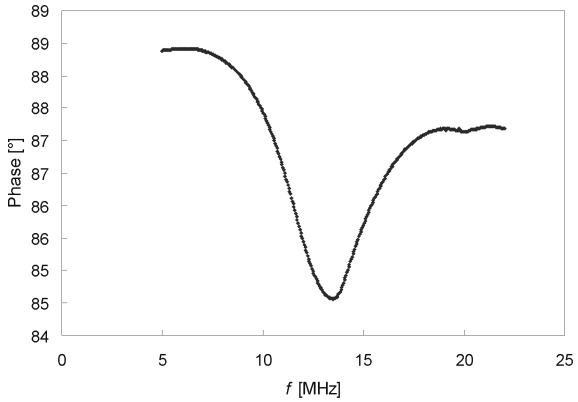

Fig.6: *Phase angle Φ of external antenna as a function of frequency for the alumina/Pt device at an operating temperature of 600 °C.*

resonance signals has been achieved at 600 °C (Fig 6). This is the limit of the temperature environment used in the testing; operation at even higher temperatures is contemplated with improved testing facilities.

ACKNOWLEDGMENTS

This work was supported in part by the Army Research Office under the Intelligent Turbine Engines MURI Program, contract number DAAH049610008, under the supervision of Dr. David Mann. Microfabrication was carried out in the Georgia Tech (GIT) Microelectronics Research Center. The authors would like to thank Ms. Jacqueline Fairley of the GIT SURE program for fabrication assistance, and Professors D. Hertling and R. Feeney of GIT for valuable technical discussion.

REFERENCES

[1] R. Okojie, A. Ned, D. Kurtz, and W. Carr, “6H-SiC pressure sensors for high temperature applications”, Proceedings of the 1996 IEEE/ASME MEMS Workshop, pp. 146-149, 1996.

[2] J.M. English, and M.G. Allen, “Wireless Micromachined Ceramic Pressure Sensors,” Proc. IEEE MEMS ’99, p. 511-516 (1999)

[3] Dupont Applied Technologies Group, “Green Tape Material System, Design and Layout Guidelines”, pp. 1-17 (available from E.I. Dupont Co.)

[4] S.P. Timeshenko, Theory of Plates and Shells, McGraw Hill, London, 1984

[5] K.L. Su, Fundamentals of Circuits, Electronics, and Signal Analysis, Houghton Mifflin Company, pp 587-614, 1978